Available online at www.sciencedirect.com

ScienceDirect

Natural Gas Industry B 2 (2015) 461–466

www.elsevier.com/locate/ngib

Research article

Experimental study on the thermostable property of aramid fiber reinforced PE-RT pipes

Qi Guoquan[a,b,*], Wu Yin[a,b], Qi Dongtao[a,b], Wei Bin[a,b], Li Houbu[a,b], Ding Nan[a,b], Cai Xuehua[a,b]

[a] *CNPC Petroleum Pipe Engineering and Technology Research Institute, Xi'an, Shaanxi 710077, China*

[b] *State Key Laboratory of Performance and Structural Safety for Petroleum Tubular Goods and Equipment Materials, 710077, China*

Received 28 May 2015; accepted 8 September 2015

Available online 28 February 2016

Abstract

Flexible composite pipes are advantageous in ultra high strength, high modulus, pH and corrosion resistance and light weight, but there are still some hidden safety troubles because they are poorer in thermostable capacity. Therefore, test samples of flexible composite pipes were prepared with high-temperature polythene (PE-RT) as the neck bush and aramid fiber as the reinforcement layer. Experimental study was conducted by using HPHT vessel and differential thermal scanner for different working conditions, different temperatures, whole-pipe pressure-bearing capacity and 1000 h viability. It is shown by the environmental compatibility test that high temperature has little effect on the weight, Vicat softening temperature, mechanical properties and structures of neck bush PE-RT, but exerts an obvious effect on the tensility and whole-pipe water pressure blasting of the reinforcement aramid fiber. Besides, the drop of whole-pipe pressure-bearing capacity is caused by deformation and breaking of aramid fibers when the reinforcement layer is under the force of internal pressure. Finally, disorientation and crystallization of molecular thermal motion occur with the rise of temperature, so amorphous orientation reduces, crystallinity factor and crystalline orientation factor increase gradually, thus, disorientation of macromolecular chains increases and tensile strength decreases. It is concluded that this type of flexible composite pipe can smoothly pass 1000 h viability test. And it is recommended that it be used in the situations with temperature not higher than 95 °C and internal pressure not higher than 4 MPa.

Keywords: Flexible composite pipe; Aramid fiber; Heat resistant polythene; Thermostable; Water pressure blasting; Pressure bearing capacity

Flexible composite pipes, also known as reinforced thermoplastic pipes (RTP), contain three layers, among which, neck bush and reinforcement layer are keys to determine mechanical and thermal properties of these pipes. In recent years, some high-performance thermo-plastics have been deployed as lining materials for flexible pipes. Accordingly, products with cross-linked polyethylene (PEX), heat-resistant polythene (PE-RT), polyvinylidene fluoride (PVDF) and polyamide (PA) as neck bush have been developed. Most of these products have polyester, aramid fiber or steel wire as reinforcing materials in the reinforcement layer [1–5]. Through copolymerization of polythene and octane, PE-RT can be produced. By controlling the quantity and distribution of side chains, unique molecular structures can be obtained to enhance the thermostable properties of PE pipes. Besides, these unique structures may significantly enhance mechanical properties, creep resistance against external stress, thermal stability, long-term hydrostatic strength, resistance to slow crack growth (SCG) and rapid crack propagation (RCP) of these materials. Aramid fibers in the reinforcement layer are characterized by ultra high strength, high modulus, pH and corrosion resistance, light weight and other outstanding properties. In addition, they have strengths 5–6 times that of

* Corresponding author. CNPC Petroleum Pipe Engineering and Technology Research Institute, Xi'an, Shaanxi 710077, China.

E-mail address: qgqstar@163.com (Qi GQ).

Peer review under responsibility of Sichuan Petroleum Administration.

http://dx.doi.org/10.1016/j.ngib.2015.09.023

steel wire, modulus twice to three times that of steel wire or glass fiber, and ductility twice that of steel wire, but weight only approximately 1/5 that of steel wire. At 560 °C, they do not decompose or melt [6–10]. With excellent insulation and aging-resistance performances, they have long life cycles. Applications of flexible composite pipes in harsh environmental conditions in oil or gas fields are confined. Heat-resistance capacities of flexible pipes are poorer than metallic pipes, and majority of flexible pipes are used in temperatures below 90 °C [11–14]. Furthermore, these pipes are characterized by a downtrend of pressure-bearing capacities with the temperature increase. Nominal pressure correction factors for different application temperatures have been proposed in relevant standards, but most of these factors are a series of fixed references determined through only limited tests (mostly with fresh water as the test medium). Consequently, these factors may not fully reflect accurate changes in temperature resistance of such pipes.

In fact, pressure correction factors for flexible composite pipes with different structures, sizes and different application media are all different [15]. Most users select reinforced thermoplastic pipes through experiments, which mainly focus on pressure-bearing capacity of pipes subject to relevant standards. For thermostable properties of pipes, only those standards for Vicat softening temperatures of thermoplastic neck bush have been applied for judgment, but performance degradation induced by variations of temperatures and pressures in later applications are not considered. Such negligence may present severe potential threats to the safe and long-term operation of such pipelines [16].

In view of this, the authors explored the thermostable properties of various layers and the whole flexible composite pipes with PE-RT as neck bush and aramid fiber as reinforcement layer. Focus was placed on the impacts of changes in temperatures on compositions and mechanical properties of neck bush and reinforcement layer.

1. Experiment

1.1. Selection of samples

Product name: aramid reinforced flexible composite pipe;
Specifications: Diameter: 100 mm; Pressure endurance: 4 MPa;
Material of neck bush: PE-RT;
Material of reinforcement layer: aramid;
Material of external protection layer: PE.

1.2. Experimental procedures

1.2.1. Performance test of material of the neck bush

By using HPHT vessel, assessments were made on materials of polythene neck bush under different working conditions, predominantly including normal temperatures and pressures, HTHP and simulated field conditions, in accordance with NACE TM 0298-2003 “Standard test method for evaluating the compatibility of FRP pipe and tubular with oilfield environments”. See Table 1 for more details related to corrosion environment and media.

Table 1
Conditions for experiments related to corrosion-resistance performances of non-metallic neck bush materials.

S/N	Test environment	Gas pressures/MPa	NaCl concentration/(mg.L^{-1})	Temperature/°C	Duration time/h
F1	Simulation of H_2S-containing conditions in an oilfield	Total pressure: 10 H_2S partial pressure: 0.60 CO_2 partial pressure: 0.25	140000	70	10 100 1000

First of all, a pipe ring with a width of approximately 15 mm was taken out of the non-metallic pipe to serve as the sample used in the experiment. The HPHT vessel was deployed to simulate the environmental conditions expected in oilfields to determine changes in weight and apparent tensile strength of the sample with different periods of test time. The apparent tensile strength can be calculated by using the following equation:

$$\sigma_a = \frac{P_b}{2A_{min}} \quad (1)$$

in which, σ_a is the tensile strength, MPa; P_b is tensile strength at break, N; A_{min} is the sectional area of the sample, mm^2.

UTM 3505 electronic universal testing machine was used to determine changes in tensile strengths of the pipe ring at different duration time (10 h, 100 h, 1000 h). Changes in weights of the samples were assessed to determine the applicability of the selected pipe in a simulated oilfield environment. XRD-300DL thermal deformation tester and Vicat softening temperature tester were used to determine the Vicat softening temperature of neck bush under the load of 50 N and at a rising room temperature rate of 50 °C/h as required in GB/T 8802-2001. Finally, Nicolet Avatar 360 Fourier Transform Infrared Spectrometer (IR) was used to determine the structures and compositions of the sample.

1.2.2. Performance test of material of the reinforcement layer

The AQ200 differential thermal scanner was used in DSC analysis. According to GB/T 14337-2008, high and low temperature test chamber was used to determine the tensile strength of the aramid fiber under different temperatures to determine the impacts of temperatures on tensile strengths.

1.2.3. Performance test of the whole pipe

1.2.3.1. Tests of whole-pipe pressure-bearing capacity. In accordance with requirements specified in SY/T 6662.2-2012, test for whole-pipe water pressure blasting was performed at room temperature and 95 °C, respectively to determine the whole-pipe pressure-bearing capacity. During the test, water bath should be used for whole pipe heating.

1.2.3.2. 1000 h viability test. According to SY/T 6794-2010, the lower confidence limit (*LCL*), maximum pressure rating (*MPR*) and maximum service pressure (*MSP*) should be determined first. See Fig. 1.

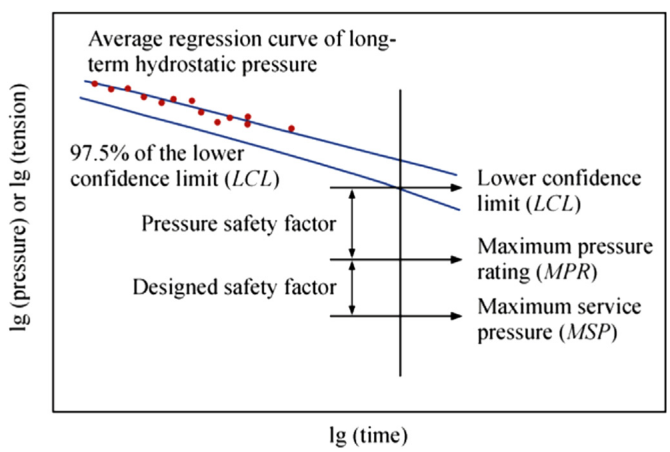

Fig. 1. Determination of *LCL*, *MPR* and *MSP*.

Sample pressure deployed in the test is 4 MPa, and accordingly, *MSP* of the pipe can be determined to be 4 MPa. The lower confidence limit (*LCL*) indicates 97.5% of predicted values are distributed above the value. The lower confidence limit of product family representative (LCL_{PFR}) is determined through extrapolation of *LCL* of the regression curve to the designed service life, which is 20 yrs. The following equations can be obtained:

$$MSP = MPR \times f_{\text{cyclic}} \times f_{\text{Fluid}} \tag{2}$$

$$MPR = LCL \times PSF \tag{3}$$

in which, default pressure safety factor (PSF) = 0.67; cyclic reduction coefficient (f_{cyclic}) = 1; fluid reduction coefficient (f_{Fluid}) = 1.

From Eq. (2) and Eq. (3), *LCL* for the designed service life 20 yrs can be determined:

$$LCL = \frac{MSP}{PSF \times f_{\text{Fluid}} \times f_{\text{cyclic}}} = \frac{4}{0.67 \times 1 \times 1} = 5.97\text{MPa} \tag{4}$$

then, linear fitting is performed in accordance with the pressures corresponding with 1 h and 20 yrs respectively to highlight the linear formula, and eventually to determine the pressure for the 1000 h viability test (δ_{1000}).

Finally, the pressure is used to perform long-term hydrostatic test to clarify if the flexible composite pipe has viability within 1000 h.

2. Results and analysis

2.1. Tests of thermostable properties of neck bush material

2.1.1. Environmental compatibility test

2.1.1.1. Changes in weights before and after corrosion. Weight of the sample increased after the compatibility test, predominantly due to swelling of the high-molecular materials after absorption of test media. The increase rate (0.38%) under simulated environment is lower than 1%, indicating that PE-RT materials displayed desirable compatibility in the simulated oilfield environment. In fact, changes in weight of the polymer materials are the results of the following two reactions: the weight increases in the sample due to the seepage of the testing media into the tested material and the weight losses due to the extraction of unconsolidated tiny resin molecules and dissolved molecules by the testing media. In addition, impacts of swelling may be higher than those of extraction of tiny molecules during the soaking of high-molecular materials, weights of the pipe samples increased slightly.

See Fig. 2 for changes in sample weights of heat-resistant polythene neck bush after tests in HPHT vessel under environmental condition of F1 (Table 1). It can also be seen that all samples have their weights increased in different media with the increase rates accelerated with increases in test durations. In general, the highest increase rates can be observed in diesel. Moreover, the increase rates are slightly higher in gas than those in solution.

2.1.1.2. Changes in apparent tensile strengths before and after corrosion. Changes in apparent tensile strengths before and after corrosion are key indicators for the corrosion-resistance

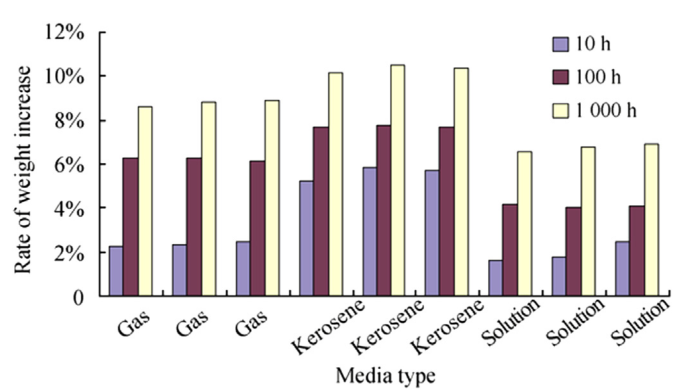

Fig. 2. Changes in rates of weight increases of PE-RT neck bush after HPHT vessel tests under environmental condition of F1.

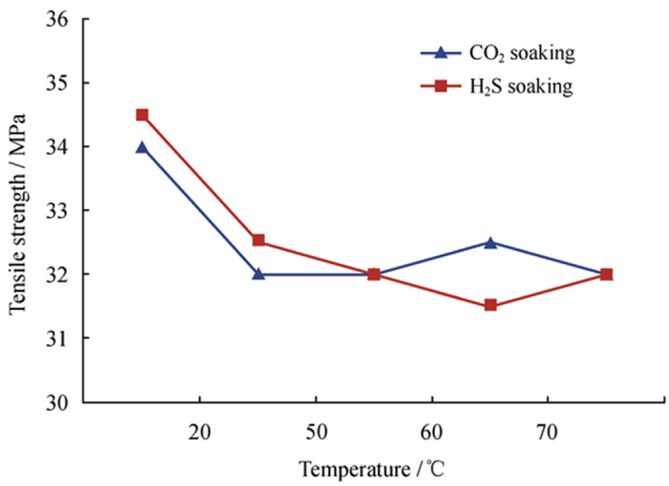

Fig. 3. Impacts of changes in temperatures on the tensility of neck bush material after corrosion.

performances of the test materials. Impacts of temperatures, pressures and media concentrations on the apparent tensile strengths of test materials will be analyzed in the following sections.

Fig. 3 shows the changes of apparent tensile strengths with temperatures before and after corrosion of the two kinds of PE neck bush materials in environments with CO_2 and H_2S, respectively. It can be seen that the apparent tensile strengths of relevant materials reduce slightly. With decrease rates below 5%, all these materials display satisfactory resistance to CO_2 and H_2S corrosion. Root causes: strengths of polyolefin materials are determined by the inherent properties of resin. With only partial swelling and basically no chemical reaction between polyolefin resin and test media, increases in temperatures have ignorable impacts on swelling. Consequently, decreases in strengths of materials with increases in temperatures are negligible [17].

Fig. 4 shows the changes in tensile strengths of the PE-RT pipe ring before and after corrosion under F1 HTHP conditions shown in Table 1. It can be seen that the tensile strengths of pipe rings decrease slightly after soaking in different media,

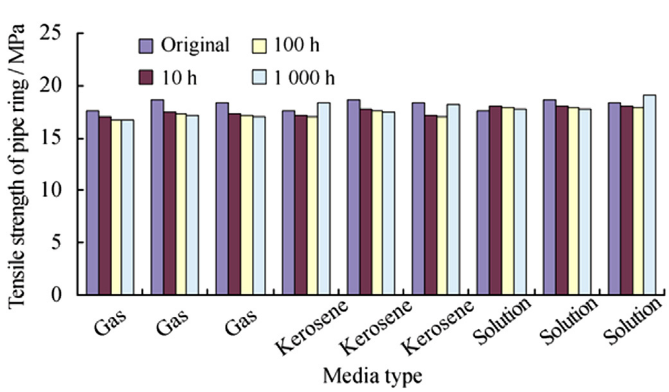

Fig. 4. Changes in tensile strength of neck bush PE-RT pipe in tests under environmental condition of F1.

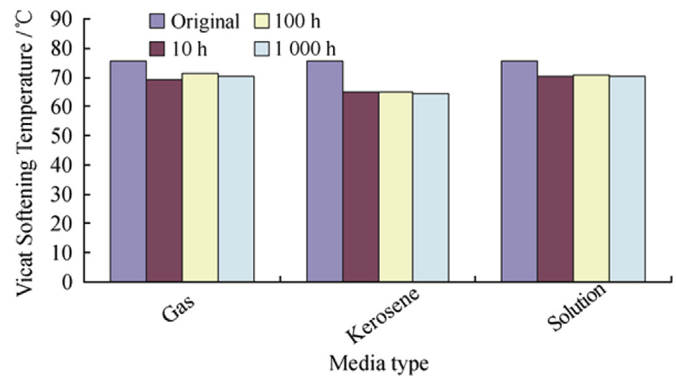

Fig. 5. Changes in Vicat softening temperatures of PE-RT neck bush in tests under environmental condition of F1.

whereas changes in tensile strengths after tests with different durations are negligible.

2.1.1.3. Changes in Vicat softening temperatures before and after corrosion. Fig. 5 shows changes in Vicat softening temperatures of PE-RT before and after corrosion under HTHP environmental conditions shown in Table 1. It can be seen that Vicat softening temperatures before and after soaking in different media all decrease slightly, whereas changes in the tensile strengths of the pipe ring after different durations are insignificant.

2.1.1.4. Changes in structures and compositions of non-metallic neck bush material. Changes in infrared spectrum before and after corrosion under HTHP environmental conditions of F1 show that relevant materials experience partial oxidization (with C–O bond broken) in the testing media, whereas changes in structures after tests with different durations are insignificant.

2.2. Performances of the reinforcement layer material

Fig. 6 shows the thermal properties of aramid fiber. It can be seen that aramid fiber experiences no significant loss in weight until the temperatures reach approximately 500 °C

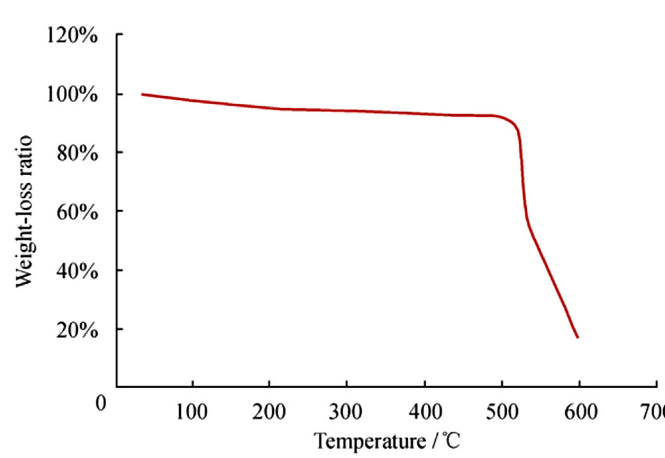

Fig. 6. Results of DSC analysis and tests of aramid fiber.

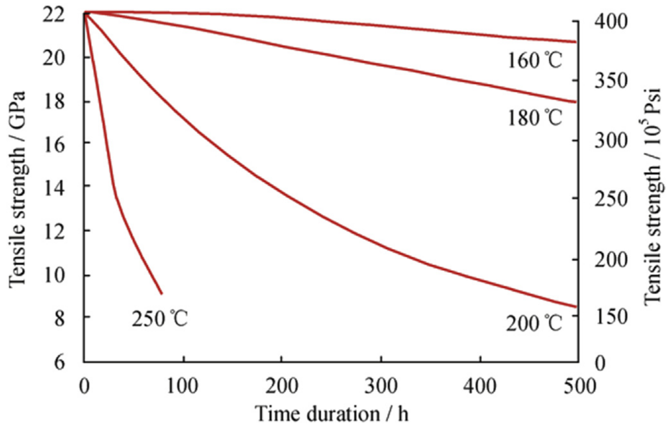

Fig. 7. Changes of tensile strengths of the aramid fiber under different temperatures. (Note: 1 psi = 6.895 kPa).

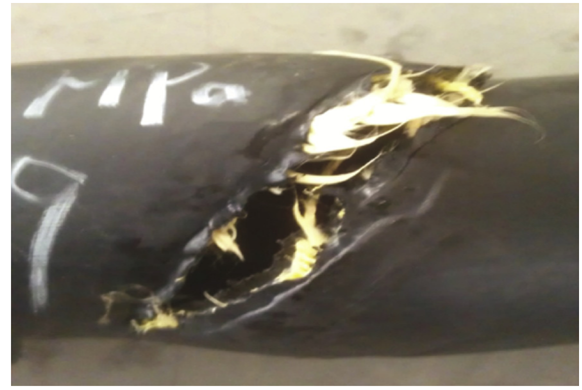

Fig. 9. Water pressure blasting failure morphology of aramid fiber reinforced pipe at 90 °C.

(with an increase rate of 10 °C/min) during DSC and thermogravimetric analysis. Accordingly, it is concluded that no pyrolysis occurred until the temperature of the aramid fiber reached 500 °C.

Fig. 7 shows the impacts of temperatures on the tensility of aramid fiber. It can be seen that the tensile strengths of the aramid fiber decrease with increases in temperatures. The higher speed temperatures increase, the faster tensile strengths decrease. Stretching of the aramid fiber can be classified into two stages: deformation and breaking. Disorientation and crystallization of molecular thermal motion occur with the rise of temperature, so amorphous orientation reduces, crystallinity factor and crystalline orientation factor increase gradually, thus, disorientation of macromolecular chains increases and tensile strength decreases [18].

2.3. Performances of whole-pipe heat resistance

2.3.1. Water-pressure blasting tests

Fig. 8 shows the changes of whole-pipe water pressure blasting pressures with changes in temperatures. It can be seen that bursting strengths of the pipe decrease with increases in temperatures. At 95 °C, the bursting strength is approximately 31% lower than that at the room temperature. But the strength can still conform to the requirements specified in SY/T 6662.2-2012 (bursting strength should be 3.0 times higher than the nominal pressure). See Fig. 9 for failure morphology of the pipe samples. Disorientation and crystallization of molecular thermal motion occur with the rise of temperature, so amorphous orientation reduces, crystallinity factor and crystalline orientation factor increase gradually, thus, disorientation of macromolecular chains increases and tensile strength decreases. With parts of large molecules broken, the pressure-bearing capacity of the composite pipe may decrease eventually.

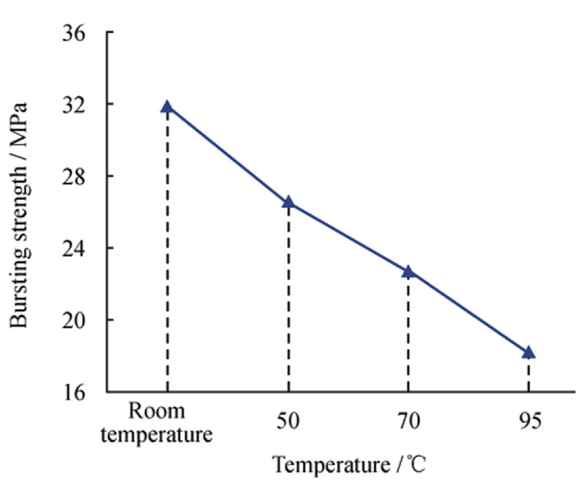

Fig. 8. Changes of water pressure blasting strength with changes in temperatures.

2.3.2. 1000 h viability test

1) First of all, it is necessary to define the test pressure of δ_{1000}. Since the aramid reinforced flexible composite pipe has a water pressure blasting strength of 18.2 MPa at 95 °C, the pressure for water pressure blasting at 95 °C for 1 h is 18.2 MPa.

2) Linear fitting can be performed in accordance with LCLs of pressures corresponding with 1 h and 20 yrs service life to highlight the linear formula $Y = -0.09X + 1.26$, from which it can be determined that $\delta_{1000} = 9.77$ MPa.

Test conditions: $\delta_{1000} = 9.77$ MPa, temperature = 95 °C. Both pipes deployed in such tests are free of leakage, crack or other forms of failure. Test results show the aramid fiber reinforced flexible composite pipe can pass the 1000 h viability test.

3. Conclusions

1) High temperature has little effect on the environmental compatibility, mechanical properties and structures of neck bush PE-RT, but exerts an obvious effect on the tensility of the reinforcement aramid fiber.

2) Under high temperature (95 °C), blasting pressures are 43% lower than that under room temperature (25 °C), but still conform to the requirements specified in relevant standards. It is concluded that this type of flexible composite pipe can

smoothly pass 1000 h viability test. It is recommended that it be used in the situations with temperature not higher than 95 °C and internal pressure not higher than 4 MPa. In addition, the flexible composite pipe can satisfy demands for a service of 20 years.

References

[1] Cai Xuehua, Qi Dongtao, Ding Nan, Fu Jiajia, Yan Miling. Failure analysis of RTP for natural gas transportation in Changqing Oilfield. In: International pipelines and trenchless technology conference. Shanghai: American Society of Civil Engineers; 2009.

[2] Yu Kuang, Morozov EV, Ashraf MA, Shankar K. Analysis of flexural behaviour of reinforced thermoplastic pipes considering material nonlinearity. Compos Struct 2015;119:385−93.

[3] Han Fangyong, Ding Jianyu, Sun Tiemin, Yang Yan. Application of the nonmetallic pipeline technologies to the oil and gas fields. Pet Plan Eng 2012;23(6):5−9.

[4] Gibson AG, Hicks C, Wright PNH, Fahrer A. Development of glass fibre reinforced polyethylene pipes for pressure applications. Plast Rubber Compos 2000;29(10):509−19.

[5] Fisher EH, Gibson AG. Continuous fibre reinforced thermoplastic pipes for transport and distribution of fluids for the oil and gas industries. Plast Rubber Compos 1999;27(10):447−51.

[6] Li Zhong, Wang Hongjun, Wei Jie. The application of plastic pipelines in oil gathering system of Tarim Oilfield. Oil Gas Storage Transp 2003;22(1):37−9.

[7] Varelidis PC, Papakostopoulos DG, Pandazis CI. Polyamide coated Kevlar™ fabric in epoxy resin: mechanical properties and moisture absorption studies. Compos Part A Appl Sci Manuf 2000;31(6):549−58.

[8] Andreopoules AG. A new coupling agent for aramid fibres. J Appl Polym Sci 1989;38(6):1053−64.

[9] Sulivan PL, Chian KS, Yue CY. Effect of bromination and hydrolysis treatments on the morphology and tensile properties of Kevlar-29 fibres. J Mater Sci Lett 1994;13(5):305−9.

[10] Lei Weiyuan, Xu Yahong, Wu Zhiwen, Lan Liwen. The adhesion and the fracture energy at the interface of composites of aramid fiber with active skin layer. Fiber Reinf Plast Compos 1996;23(1):35−7.

[11] Kruijer MP, Warnet LL, Akkerman R. Analysis of the mechanical properties of a reinforced thermoplastic pipe (RTP). Compos Part A Appl Sci Manuf 2005;36(2):291−300.

[12] Conley J, Weller B, Slingerland E. The use of reinforced thermoplastic pipe in oil and gas gathering and produced water pipelines. In: CIPC/SPE Gas technology symposium 2008 joint conference, 16−19 June 2008, Calgary, Alberta, Canada. http://dx.doi.org/10.2118/113718-MS.

[13] Reis JML, Chaves FL, da Costa Matto HS. Tensile behavior of glass fibre reinforced polyurethane at different strain rates. Mater Des 2013;49:192−6.

[14] Qi Dongtao, Ren Jianhong, Li Houbu, Ren Penggang, Zhang Hua. The permeation law of hydrogen sulfide in multilayer polymer composite oil/gas pipes. Nat Gas Ind 2014;34(5):126−30.

[15] Humpenodre J. Gas permeation of fiber reinforced plastics. Cryogenics 1998;38(1):143−7.

[16] Young RJ, Bannister DJ, Cervenka AJ, Ahmad I. Effect of surface treatment upon the pull-out behavior of aramid fibres from epoxyresins. J Mater Sci 2000;35(8):1939−47.

[17] Banduryan SI, Iovleva MM, Zhuravleva AI, Shchetinin AM, Machalaba NN, Budnitskii GA. Genesis of the surface structure of Armos fibre. Fibre Chem 2002;34(6):422−5.

[18] Kotomin SV, Avdeev NN. Compaction and consolidation of aramid and composite fibers. Mech Compos Mater 2002;38(5):461−70.